Appl Phys B (2011) 102: 497–502
DOI 10.1007/s00340-011-4408-4

Applied Physics B
Lasers and Optics

Towards T_1-limited magnetic resonance imaging using Rabi beats

H. Fedder · F. Dolde · F. Rempp · T. Wolf · P. Hemmer · F. Jelezko · J. Wrachtrup

Received: 1 September 2010 / Revised version: 20 December 2010 / Published online: 11 February 2011

Abstract Two proof-of-principle experiments toward T_1-limited magnetic resonance imaging with NV centers in diamond are demonstrated. First, a large number of Rabi oscillations is measured and it is demonstrated that the hyperfine interaction due to the NV's ^{14}N can be extracted from the beating oscillations. Second, the Rabi beats under V-type microwave excitation of the three hyperfine manifolds is studied experimentally and described theoretically.

1 Introduction

The ever increasing need for high resolution imaging in the life sciences, material science, and more recently quantum information processing, has led over the past decade to the development of a variety of methods that try to overcome the limits set by optical diffraction [13]. Exploiting the nonlinear behaviour of fluorescent labels, a spatial resolution down to few nanometers was demonstrated using optical techniques such as STED [7], PALM [3], and STORM [15]. A technique whose resolution is independent of the wavelength is magnetic resonance imaging. Magnetic resonance imaging and nanoscale magnetic and electric field sensing are key technologies in various areas of science. Recently, magnetic resonance imaging as well as scanning probe magnetic imaging on scales relevant to molecular biological processes was demonstrated [1, 9]. A spin label that is suitable for high resolution measurements are nitrogen vacancy centers embedded in diamond nanocrystals [19]. Owing to their optical addressability, photostability, and long spin coherence time, recently sub 10 nm spatial resolution as well as the detection of magnetic fields close to individual electron spins has been demonstrated using NV nano sensors [1, 9]. The spatial resolution of a magnetic resonance measurement is determined by the strength of the field gradient and the effective linewidth of the electron spin transition. Pulsed imaging modes, such as the Hahn–Echo and Carr–Purcell–Meiboom–Gill (CPMG) [10] sequence can be used to decrease the effective linewidth. The continuous driving of Rabi oscillations has been proposed to decrease the effective linewidth down to the limit given by the spin decay time [18]. In this paper, we perform a proof-of-principle study of this imaging mode. The feasibility of the method is demonstrated by resolving the hyperfine interaction of the NV center due to its ^{14}N nuclear spin.

In the simplest magnetic resonance imaging mode, a CW electron spin resonance (ESR) measurement is performed, and the effective linewidth is given by the inhomogenously broadened spin de-coherence time T_2^*, which is typically short and only of the order of few microseconds in case of the NV center. In the Hahn–Echo sequence, $\pi/2 - \pi - \pi/2$ pulses are used to refocus precessing spins, such that noise generated by slowly fluctuating spins in the environment is canceled. For the Hahn–Echo sequence, the effective linewidth is given by the dephasing time T_2 of the spin system, which is larger than T_2^*, and can reach several hundred microseconds in the case of the NV center [2]. More advanced pulse sequences, such as the CPMG sequence, hold promise to decrease the effective linewidth even further [5, 11, 16]. Another elegant imaging mode is based on the continuous driving of Rabi oscillations. The

H. Fedder (✉) · F. Dolde · F. Rempp · T. Wolf · F. Jelezko · J. Wrachtrup
3rd Physics Institute and Research Center SCoPE, University of Stuttgart, Pfaffenwaldring 57, 70550 Stuttgart, Germany
e-mail: helmut.fedder@gmail.com

P. Hemmer
Department of Electrical and Computer Engineering, Texas A&M University, College Station, TX 77843, USA

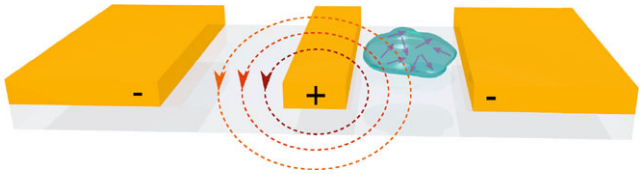

Fig. 1 Principle of magnetic resonance imaging based on Rabi beats

decay time of Rabi oscillations depends on the microwave power and is similar to the decay time observed in a spin locking experiment. The exact decay time is determined by the noise spectral density at the Rabi frequency and for the typical $1/f$-Noise, and assuming that the Rabi frequency does not accidentally coincide with a peak in the noise spectral density—such as ^{13}C Larmor peak or other discrete spin noise—it is expected to approach T_1 as the Rabi frequency becomes close to the transition frequency. Note that at the transition frequency, the rotating wave approximation starts to break down. Among the various magnetic resonance imaging modes, this mode may potentially achieve a particularly long decay time, and thus high spatial resolution. Over the past years, there has been a continued effort to apply this magnetic resonance imaging mode to the NV center [18]. However, this poses great challenges. In this mode, spatial information is extracted from beat frequencies observed in the Rabi oscillations. A high spatial resolution requires the measurement of a large number of Rabi oscillations. Here, we demonstrate the feasibility of this imaging mode by realising the measurement of a large number (>500) of Rabi oscillations, and resolve the hyperfine splitting due to the NV's ^{14}N nuclear spin from the Rabi beats. Moreover, we investigate experimentally and describe theoretically the observed Rabi beats in case of a V-type energy level scheme, which is the desired excitation mode in a high resolution experiment.

The principle of magnetic resonance imaging using Rabi beats is illustrated in Fig. 1. We envision a sample, such as a living cell, that is tagged with nano diamonds that contain single NV centers. The NV electron spins are initialized and read out optically using a confocal microscope. An inhomogeneous microwave field—such as the one generated by a coplanar waveguide—is applied to the sample. The microwaves are matched to the $m_s = 0 \rightarrow \pm 1$ electron spin transition and drive Rabi oscillations between the ground-state spin sub-levels. The Rabi frequency depends on the microwave power, thus encoding the position within the microwave field. From an a priori knowledge of the microwave field (or from a reference measurement), the position of the individual NV centers with respect to the electrodes can be determined. To obtain the NV position in two spatial directions as well as the angle of the NV center, successive measurements are performed with microwave gradients applied in different directions using a two-dimensional waveguide structure.

In this magnetic resonance imaging mode, the resolution is given by the decay time τ of the Rabi oscillations, the Rabi frequency Ω, and the strength of the microwave gradient. The number N of observable Rabi oscillations is linked to τ and the Rabi frequency as

$$\frac{\Omega\tau}{2\pi} = N. \tag{1}$$

For the present coplanar waveguide, the field gradient is determined by the width G of the gap, and the resolution δx follows approximately as

$$\delta x = \frac{G}{N}. \tag{2}$$

The maximum achievable Rabi frequency is of the order of the Larmor frequency of the spin [4]. In this case, the decay time τ of the Rabi signal becomes T_1 and the resolution approaches

$$\delta x = \frac{2\pi G}{T_1 \Omega}, \tag{3}$$

where $\Omega = \omega = D \approx 2.88$ GHz is equal to the electron spin transition. For NV centers, the T_1 time is typically few ms at room temperature [14], such that a product $T_1\omega = 10^6$ could in principle be achievable. With $G = 10$ μm a spatial resolution of 0.01 nm would be reached. However, this poses stringent requirements on the stability of the applied microwave field. Both the power stability and the spatial stability of the microwave field (expressed as a relative error) should be at least as small as $1/(T_1\Omega)$, and to achieve sub-Angstrom resolution; the microwave wire should not drift by more than a fraction of an atomic diameter. Since the Rabi frequency is determined by the component of the microwave's magnetic field vector along the NV magnetic dipole axis, the Rabi frequency depends on the orientation of the NV. Thus a practical imaging experiment requires several measurements with different field configurations of the applied microwaves. While this experiment requires an increased amount of resources, this measurement scheme is suitable to determine both the position and the orientation of the NV center. For imaging with NV active nano diamonds, in addition the strain splitting (which differs from crystal to crystal and typically amounts to tens of MHz) has to be carefully calibrated, e.g., by several measurements with and with an applied DC bias magnetic field.

2 Results and discussion

To demonstrate the observation of Rabi beats, we study a single NV center in a fixed microwave field. Rabi beat measurements with a single NV center are possible owing to hyperfine interaction of the electron spin with the ^{14}N nuclear

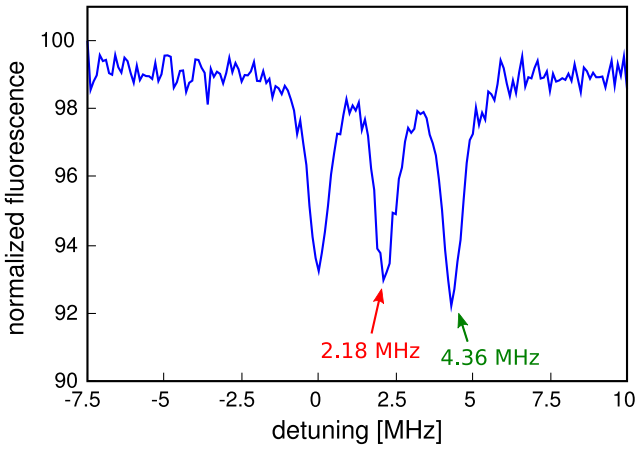

Fig. 2 ESR spectrum of the NV center showing the hyperfine splitting of the $m_s = 0 \rightarrow -1$ spin level due to ^{14}N. The spectrum was recorded with an applied DC magnetic field of about 150 G. Detuning is denoted relative to the lowest hyperfine transition corresponding to 2.4524 GHz

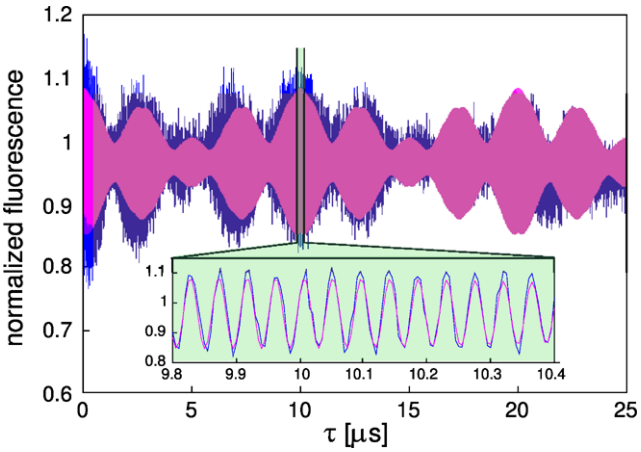

Fig. 3 Electron spin Rabi oscillations. *Solid blue line*: experimental data, *solid magenta line*: result from Fourier transform (Fig. 4). Three beating cosine with frequencies corresponding to the three local maxima in the FFT are plotted

spin that results in a splitting of the groundstate spin manifold into three hyperfine sub-levels. Each hyperfine transition has a slightly different Rabi frequency, which results in a beat signal in the measured Rabi oscillations. These hyperfine beats will also be seen in high resolution Rabi beat imaging data as a modulation, and it is important to identify and assign them correctly. Here, we are interested in the hyperfine interaction caused by the ^{14}N nucleus (nuclear spin $J = 1$) of the NV center, which splits the $m_s = \pm 1$ ground state spin levels each into three hyperfine sub-levels with an energy splitting of $\delta_{^{14}\mathrm{N}} \approx 2.18$ MHz. This energy splitting is seen in the CW electron spin resonance (ESR) measurement shown in Fig. 2. In here, the ESR measurement is performed on the $m_s = 0 \rightarrow -1$ electron spin transition. Zero de-tuning corresponds to a driving microwave field of 2.4524 GHz. Note that a permanent magnetic field with a component along the NV axis of about 150 G has been applied to shift the $m_s = 0 \rightarrow -1$ transition away from its zero field value (2.88 GHz) owing to the Zeeman effect, and thus to separate it from the $m_s = 0 \rightarrow +1$ spin transition (which is shifted to higher frequency of 3.3 GHz). This separation between the two electron spin transitions is necessary in order to ensure that the strong microwave field does not simultaneously drive both spin manifolds.

We now consider the Rabi beats expected for the given hyperfine splitting. For a driving microwave field that is detuned by a small frequency δ from the resonant transition, the Rabi frequency Ω is increased as compared to the resonant Rabi frequency Ω_0, following [17]

$$\Omega = \sqrt{\Omega_0^2 + \delta^2}. \tag{4}$$

For small detuning ($\delta \ll \Omega_0$), the shift of the Rabi frequency $\delta\Omega$ becomes

$$\delta\Omega = \frac{\delta^2}{2\Omega_0}. \tag{5}$$

Suppose the microwave frequency corresponds to the lowest hyperfine transition (as in the present experiments). In this case, the lowest hyperfine transition is driven with Rabi frequency Ω_0, while the two other hyperfine transitions are driven with faster Rabi frequencies corresponding to detunings $\delta_0 = 2.18$ MHz and $\delta_{-1} = 4.36$ MHz. Using (4), we can evaluate the expected Rabi frequencies. The resulting signal is the sum of three oscillations, whose frequencies can be extracted by Fourier transformation. Also, the three frequencies result in several beat frequencies in the Rabi signal.

To measure Rabi beats, a coplanar waveguide (gap = 10 μm, width = 10 μm) was fabricated directly onto a type IIa diamond sample with ⟨100⟩ crystallographic orientation and less than 4 ppb nitrogen concentration (element6, electronic grade). A DC magnetic field was applied with a permanent magnet. A microwave field resonant to the lowest of the hyperfine transitions (2.4524 GHz) was generated with a synthesizer (Rhode&Schwarz SMIQ) and applied to the sample through a fast switch (mini-circuits ZASW-2-50DR). A single NV center was identified in the coplanar gap using a home built confocal fluorescence microscope. Rabi oscillations were measured using a standard laser and microwave pulse sequence [8]. Figure 3 shows the corresponding Rabi oscillations. The data shows a base oscillation of about 42 MHz (see inset). Due to the beating this is approximately twice the base Rabi frequency. The two beat frequencies $\delta\Omega_0 = 100$ kHz and $\delta\Omega_{+1} = 400$ kHz correspond to the $m_s = 0$ and $m_s = +1$ hyperfine transition. Thus, in total, three Rabi oscillations are observed.

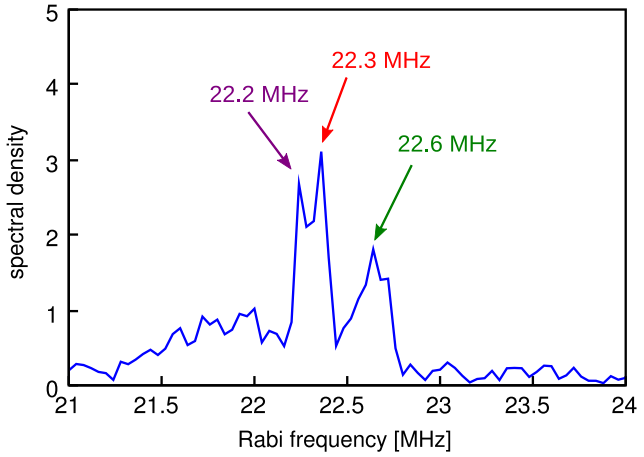

Fig. 4 Fourier transform of the Rabi signal. The data shows three distinct Rabi frequencies corresponding to the individual hyperfine levels

Their individual frequencies are seen in the Fourier transform (Fig. 4) that shows $\Omega_{-1} = 22.2$ MHz, $\Omega_0 = 22.3$ MHz, and $\Omega_{+1} = 22.6$ MHz. Note that the FFT data shows less pronounced peaks due to the relatively sparse sampling of less then 10 points per period (see also zoom in Fig. 3) and power drift during the measurement. The sparse sampling was necessary to keep the total measurement time (several days for Fig. 3) within reasonable bounds. To complete our measurement of the hyperfine splitting from the Rabi beats, we use (5) and convert the measured beats into energy level shifts. We find $\delta_0 = 2.1$ MHz and $\delta_{-1} = 4.2$ MHz, which is in good agreement with the ESR spectrum (Fig. 2).

The Rabi oscillations show a decay at about 25 µs, which is much smaller than T_1. We tentatively attribute this to microwave power drift. In this case, the resolution of the hyperfine measurement is as follows. We denote the experimentally observed decay constant by τ. The resolution of a hyperfine measurement from the Rabi beats is determined by the Rabi frequency and the number N of visible Rabi oscillations. To measure a small change in the Rabi period T, we need to measure a large number of oscillations. Combining (1) with (5), we have

$$\delta = \frac{\Omega}{\sqrt{N}} = \frac{2\pi}{\sqrt{\tau T}}. \tag{6}$$

In our case, we find $\delta \approx 6$ MHz, which is in good qualitative agreement with our observations, since our data, in particular the Fourier transform, Fig. 4, shows that we can indeed resolve the 4.32 MHz detuning related to the farther detuned hyperfine level (22.6 MHz peak in the FFT), however, we can just barely resolve the 2.16 MHz detuning related to the lesser detuned hyperfine level (22.3 MHz peak in the FFT). In the present measurements, the total number of Rabi oscillations is about 500, which translates into an equivalent spatial resolution of about 10 nm. We expect that an improvement of the power stability to a level better than 10^{-4} should be achievable without a large technical effort, and that spatial drifts of the microwave field should still be negligible in this case. Thus, a spatial resolution of about 1 nm is feasible.

For a high resolution imaging experiment, a large number of Rabi oscillations, and thus a fast Rabi frequency is required. In this case, it is no longer feasible to shift the $m_s = \pm 1$ spin levels sufficiently far apart from each other such that a single spin transitions is driven selectively. This is because the separation between the $m_s = \pm 1$ levels needed to be larger than the Rabi frequency. This would in turn require a large magnetic field. However, at a large magnetic field, level mixing causes the optical ESR contrast to vanish, unless the magnetic field is aligned parallel to the NV axis [12]. Alignment of the magnetic field parallel to the NV axis is, however, not possible in a sample with many randomly distributed NV centers. Thus, in a high resolution measurement, we will always measure with a small DC bias field, and hence we will simultaneously drive the $m_s = \pm 1$ spin transitions. In this case, six hyperfine levels are present whose Rabi oscillations beat with each other. This situation differs from the previous experiments. While in the previous case, the Rabi signal was an incoherent sum of three oscillations (during a measurement, the nuclear spin switched randomly and slowly between the different spin states), now each nuclear spin manifold forms a V-type energy level scheme that is driven simultaneously. In the following, we evaluate the corresponding Rabi beat signal.

The NV's spin Hamiltonian with external magnetic field reads (for a recent discussion of the electronic structure as well as ground state spin Hamiltonian, see, e.g., [6])

$$H = \mathbf{H}_{\mathrm{ZFS}} + \mathbf{H}_{\mathrm{Z}} \tag{7}$$

with

$$\mathbf{H}_{\mathrm{ZFS}} = D\left(\mathbf{S}_z^2 - \frac{2}{3}\mathbb{1}\right) + E(\mathbf{S}_x^2 - \mathbf{S}_y^2) \tag{8}$$

$$\mathbf{H}_{\mathrm{Z}} = \frac{g\,\mu_B}{h}\,B\,\mathbf{S}_z, \tag{9}$$

where D is the zero field splitting and E is the strain splitting. We transform into the energy eigenbasis and denote the $m_s = 0$ state as $|0\rangle$ and the two states that correspond to the $m_s = \pm 1$ states as $|1\rangle$ and $|2\rangle$. The interaction of the spin system with the microwave field is treated using the semi-classical approximation, expressed by the Hamiltonian

$$\mathbf{H}_{\mathrm{MW}} = \Omega_0\,\mathrm{e}^{\mathrm{i}\omega t}\,\mathbf{S}_x, \tag{10}$$

where ω is the microwave frequency and Ω_0 is the Rabi frequency. Here, we assume that both transitions have the same transition matrix elements, which is justified for typical strain splittings E observed in experiment, which are

of the order 100 kHz. We apply the rotating wave approximation (RWA) and transform into the rotating frame, which leaves us with the Hamiltonian

$$\mathbf{H}_{\text{rot}} = \begin{pmatrix} 0 & \Omega_0 & \Omega_0 \\ \Omega_0 & \Delta - \delta' & 0 \\ \Omega_0 & 0 & \Delta + \delta' \end{pmatrix}, \tag{11}$$

where $\delta' = \Delta E_{|1\rangle\,|2\rangle}/2$ and Δ the detuning of the microwave from $|1\rangle + \delta'$.

To obtain an analytical solution, we set $\Delta = 0$. Calculation of the eigenvalues leads to the Rabi frequency $\Omega' = \sqrt{2\,\Omega_0^2 + \delta'^2}$. Considering that $\Omega_0 \gg \delta'$, we see that the Rabi frequency is $\sqrt{2}$ times faster, as compared to the case of driving a single level. We now consider the time evolution of the system with initial state $|0\rangle$. The dynamics of $|0\rangle$ are

$$\rho_{|0\rangle} = \frac{(\delta'^2 + 2\Omega_0^2 \cos[\sqrt{2\Omega_0^2 + \delta'^2}t])^2}{(2\Omega_0^2 + \delta'^2)^2}. \tag{12}$$

The expression indicates, that there are actually two oscillation frequencies involved, corresponding to the cos and $\cos^2$ terms. Appreciating that $\Omega_0 \gg \delta'$, we see that the dominant term is the $\cos^2$ term, whereas the cos term represents an additional small signal. The former will represent the base Rabi frequency observed in experiments and will generate beat signals. Using a standard trigonometric identity, we find the expression for the Rabi frequency

$$\Omega' = 2\sqrt{2\Omega_0^2 + \delta'^2}, \tag{13}$$

with base frequency $\Omega_0' = 2\sqrt{2}\Omega_0$ and a detuning term $2\delta'$. Approximating the square root to leading order, we find

$$\delta\Omega' = \frac{2\delta^2}{\Omega_0'}. \tag{14}$$

Note the additional factor 4 as compared to the expression for the standard case with non-V-type driving given in (5).

To measure Rabi beats with V-type microwave excitation, we remove the DC bias field. Moreover, we pick a different NV center that is closer to the central conductor and feels a higher microwave power. Figure 5 shows the ESR spectrum, with a total of five dips. The central dip is about twice larger as compare to the other dips. In this experiment, the Zeeman splitting due to a residual magnetic field (earth magnetic field as well as magnetized parts of the setup) closely matches the hyperfine splitting. As a consequence, the two hyperfine triplets corresponding to the $m_s = -1$ and $m_s = +1$ spin transition are shifted in such a way that the highest transition of the lower triplet overlaps with the lowest transition of the higher triplet, resulting in a total five dips with a pronounced central dip. Rabi oscillations are

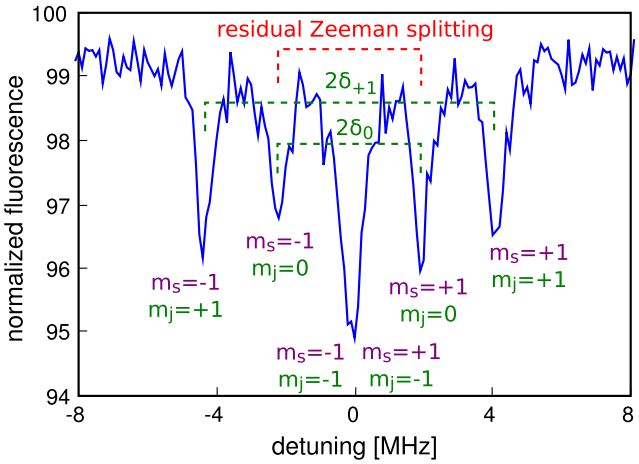

Fig. 5 ESR spectrum of the second NV center without DC bias field. The two hyperfine triplets corresponding to the $m_s = -1$ and $m_s = +1$ spin levels overlap in the central dip. Detuning is denoted relative to the central hyperfine transition corresponding to 2.8706 GHz

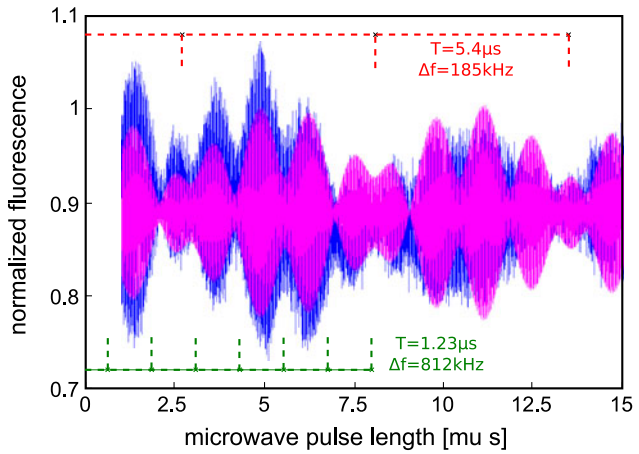

Fig. 6 Rabi oscillations under V-type microwave excitation. *Solid blue line*: experimental data. *Red* and *green markers* denote the extracted beat frequencies. *Solid magenta line*: result of the extracted beat frequencies. Three beating cosine with the corresponding frequency shifts are plotted

now driven with the microwave frequency tuned in resonance with the central dip corresponding to 2.8706 GHz. This case corresponds to the theoretical case $\Delta = 0$ treated above, with $\delta_0 = 2.18$ MHz and $\delta_{+1} = 4.36$ MHz for the driving of the $m_j = 0$ and $m_j = +1$ manifold, respectively.

The Rabi oscillations and their Fourier transform are shown in Figs. 6 and 7. The first observation is that the Rabi frequency is increased by about a factor of two as compared to the previous case. Two effects contribute here. First, with V-type driving, the Rabi frequency is enhanced by a factor of $\sqrt{2}$ as compared to driving a single transition, and second, the Rabi frequency is additionally increased due to the higher microwave power in the close vicinity of the central conductor. The second observation is a fast and a slow beat

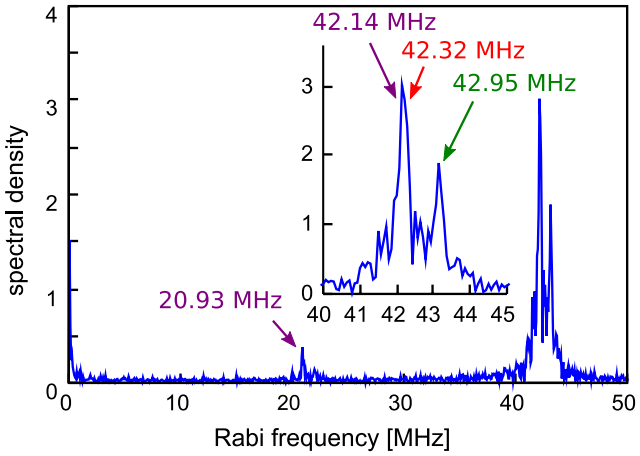

Fig. 7 Fourier transform of the Rabi oscillations under V-type microwave excitation. Peaks around 42 MHz and 21 MHz correspond to the base Rabi oscillations and a modulation at half the frequency. The *inset* shows the beating Rabi frequencies around 42 MHz. Labels mark the three frequencies as extracted from the beat analysis of the raw data. The FFT resolves the fast beat, while it does not resolve the slow beat due to sparse sampling

with frequency of about 185 kHz and 812 kHz, respectively. These beats are seen most clearly in the Rabi oscillations. Note that the slower beat is not resolved in the FFT (Fig. 7) due to power drift and sparse sampling. We can now convert the observed beatings to energy level shifts. According to (14) we find $\delta_0 = 2.0$ MHz and $\delta_{+1} = 4.1$ MHz, which is in good agreement with the ESR spectrum. We also observe the expected weak peak at half the base Rabi frequency (21 MHz) corresponding to the cos term evaluated in (12).

3 Summary and conclusions

We have performed two proof-of-principle experiments towards T_1 limited magnetic resonance imaging with NV centers in diamond. First, we have demonstrated the measurement of a large number (>500) of Rabi flops, and we have shown that the hyperfine interaction due to ^{14}N can be resolved from such a measurement. Second, we have studied the Rabi beats without a large DC bias field, where the nuclear spin manifolds form V-type energy level schemes. The base Rabi frequency is increased by $\sqrt{2}$ and the time evolution of the state population is modulated by an oscillation with half the base Rabi frequency. While the present experiments were performed in bulk, in the future, it will be an important step to demonstrate Rabi beat imaging with NV centers embedded in diamond nanocrystals. The present experiments are relevant to quantum information processing in diamond. The ability to drive a large number of Rabi flops could allow to precisely control the spin state of several (detuned) NV centers simultaneously. We envision a microwave pulse with precisely adjusted length that performs independent unitary transformations on a quantum register, such as rotate an NV A to $|1\rangle$ while simultaneously rotating an NV B to the superposition $\sqrt{2}(|0\rangle + |1\rangle)$.

Acknowledgements This work was supported by the EU (QAP, EQUIND, NEDQIT, SOLID), DFG (SFB/TR21, FOR730 and FOR1482), NIH, Landesstiftung BW, BMBF (EPHQUAM, KEPHOSI), and Volkswagen Stiftung

References

1. G. Balasubramanian, I.Y. Chan, R. Kolesov, M. Al-Hmoud, J. Tisler, C. Shin, C. Kim, A. Wojcik, P.R. Hemmer, A. Krueger et al., Nature **455**, 648 (2008)
2. G. Balasubramanian, P. Neumann, D. Twitchen, M. Markham, R. Kolesov, N. Mizuochi, J. Isoya, J. Achard, J. Beck, J. Tissler et al., Nat. Mater. **8**, 383 (2009)
3. E. Betzig, G.H. Patterson, R. Sougrat, O.W. Lindwasser, S. Olenych, J.S. Bonifacino, M.W. Davidson, J. Lippincott-Schwartz, H.F. Hess, Science **313**, 1642 (2006)
4. I. Chiorescu, Y. Nakamura, C. Harmans, J.E. Mooij, Science **299**, 1869 (2003)
5. G. de Lange, Z.H. Wang, D. Ristè, V.V. Dobrovitski, R. Hanson, Science **330**, 60 (2010)
6. M.W. Doherty, N.B. Manson, P. Delaney, L.C.L. Hollenberg, The negatively charged nitrogen-vacancy centre in diamond: the electronic solution. Arxiv preprint, arXiv:1008.5224 (2010)
7. S.W. Hell, J. Wichmann, Opt. Lett. **19**, 780 (1994)
8. F. Jelezko, T. Gaebel, I. Popa, A. Gruber, J. Wrachtrup, Phys. Rev. Lett. **92**, 76401 (2004)
9. J.R. Maze, P.L. Stanwix, J.S. Hodges, S. Hong, J.M. Taylor, P. Cappellaro, L. Jiang, M.V.G. Dutt, E. Togan, A.S. Zibrov et al., Nature **455**, 644 (2008)
10. S. Meiboom, D. Gill, Rev. Sci. Instrum. **29**, 688 (1958)
11. B. Naydenov, F. Dolde, L.T. Hall, C. Shin, H. Fedder, L.C.L. Hollenberg, F. Jelezko, J. Wrachtrup, Dynamical Decoupling of a single electron spin at room temperature. arXiv:1008.1953 (2010)
12. P. Neumann, J. Beck, M. Steiner, F. Rempp, H. Fedder, P.R. Hemmer, J. Wrachtrup, F. Jelezko, Science **329**, 542 (2010)
13. A. Pertsinidis, Y. Zhang, S. Chu, Nature **466**, 647 (2010)
14. D.A. Redman, S. Brown, R.H. Sands, S.C. Rand, Phys. Rev. Lett. **67**, 3420 (1991)
15. M.J. Rust, M. Bates, X. Zhuang, Nat. Methods **3**, 793 (2006)
16. A. Schweiger, G. Jeschke, *Principles of Pulsed Electron Paramagnetic Resonance* (University Press, Oxford, 2001)
17. M.O. Scully, M.S. Zubairy, *Quantum Optics*, 3rd edn. (Cambridge University Press, Cambridge, 1999)
18. C. Shin, C. Kim, R. Kolesov, G. Balasubramanian, F. Jelezko, J. Wrachtrup, P.R. Hemmer, J. Lumin. **130**, 1635 (2010)
19. J. Tisler, G. Balasubramanian, B. Naydenov, R. Kolesov, B. Grotz, R. Reuter, J.P. Boudou, P.A. Curmi, M. Sennour, A. Thorel et al., ACS Nano **3**, 1959 (2009)